Journal of the Brazilian Society of Mechanical Sciences and Engineering (2021) 43:551
https://doi.org/10.1007/s40430-021-03276-y

TECHNICAL PAPER

On the prediction of strength and deformation anisotropy of automotive sheets for stamping formability analysis

Emre Esener[1] · Toros Arda Akşen[2] · Aysema Ünlü[1] · Mehmet Firat[2]

Received: 7 July 2021 / Accepted: 9 November 2021 / Published online: 22 November 2021

Abstract
Today, sheet metal process simulations based finite element (FE) analysis became an indispensable part of tool design engineering in automotive and related stamping industries. In this context, an analytical description of the inherent directional strength and deformation variations in these sheet metals are conducted by means of an orthotropic yield criterion. In practice, an appropriate criterion can be determined using directionality parameters such as r-values and yield stress ratios from simple tension tests to predict material strength and deformation anisotropies analytically. When yield criteria together with the computed anisotropy parameters are implemented into the finite element software, however, it should be also investigated whether the finite element (FE) model could capture the actual anisotropic behavior of the material and assess the analytical model accurately. One way of ensuring this condition is to use single finite element tests in order to simulate uniaxial deformation behavior of material in simple tensile tests. In this study, FE analyses of simple tension test with sheet specimens were conducted for specimens from seven evenly spaced directions for two widely used sheets in the automotive industry, namely DP600 and AA2090-T3 aluminum alloy. Lankford parameters and the yield stress ratios were predicted with analytical approach and FE analysis for different material orientations. It is determined that, while plasticity model analyses are quite successful in terms of computed deformations and flow curves, Barlat's yield functions family has significant strength and deformation differences between analytical and numerical results, especially for steel sheets. It is assessed that these discrepancies are caused by plasticity implementation into FE software.

Keywords Stamping · Formability · Plasticity · Automotive sheets · Finite elements

1 Introduction

Today, the increasing use of lightweight materials plays an important role in the automotive industry in order to meet ever-decreasing environmental pollution and fuel consumption restrictions. Aluminum alloys and advanced high strength steels (AHSS) have become prominent choices in these regards due to their weight/strength ratio advantage. For this reason, accurate plasticity modeling is a critical step for these materials, especially for finite element analyses. A plasticity model comprises a yield criterion, flow rule, and hardening rule. The yield criterion represents a boundary known as a yield locus separating the elastic and plastic regions from each other in stress space, and material anisotropy affects the shape of this boundary [1]. In addition, the yield criterion is considered as the plastic potential for flow rule, which is used to determine the direction of the incremental plastic strain. In this regard, modeling of the material anisotropy is also essential to determine the plastic strain increments. In the literature, several material models were proposed to describe the anisotropic behavior of the material. The first anisotropic yield criterion was proposed by Hill [2]. This famous yield function is prevalently used and has six parameters to be calibrated. Besides, this criterion (Hill-48) is quite useful for steel. Chung et al. [3] performed hole expansion simulations of three different steel grades, including advanced high strength steels (AHSS) using Hill's criterion. These steels are namely, 340R, TRIP590, and TWIP940. It was concluded that the obtained results were

Technical Editor: João Marciano Laredo dos Reis.

✉ Mehmet Firat
firat@sakarya.edu.tr

[1] Mechanical Engineering Department, Bilecik Seyh Edebali University, Bilecik, Turkey

[2] Mechanical Engineering Department, The University of Sakarya, Serdivan, Sakarya, Turkey

in good agreement with the experimental results. On the other hand, this criterion is not recommended for aluminum alloys. The reason is that this criterion cannot model the first and second-order anomalous behaviors. The first-order anomalous behavior was firstly reported by Woodthorpe and Pearce [4]. They observed that several materials, especially aluminum alloys, have an average anisotropy coefficient less than 1 but they have balanced biaxial yield stress higher than the uniaxial yield stress. For these materials, the yield locus is outside of the von Mises ellipse. Hill's criterion cannot model this behavior hence, in nature, this criterion leads to a yield locus prediction located inside of the von Mises ellipse when the average anisotropy coefficient is less than 1. Second anomalous behavior was reported by Banabic et al. [5]. They observed that some materials having a ratio of yield stress in rolling direction to that of transverse direction higher than 1, have a ratio of r-value in rolling direction to that of in transverse direction less than 1 (or vice versa). However, Hill's criterion predicts both ratios, either higher or lower than 1. To describe both anomalous behaviors in addition to biaxial yield stress, a yield function should accurately predict the yield stresses and r values in rolling and transverse directions. In order to overcome the anomalous issue reported by Woodthorpe and Pearce, Hill also proposed several different anisotropic yield criteria [6–8]. Among them, Hill (1979) criterion overcomes the first order anomalous issue, Hill (1993) criterion overcomes both the first and second anomalous problems; however, these criteria do not take the shear components into account [6, 9]. On the other hand, despite Hill (1990) criterion overcomes both first and second-order anomalous behaviors, it suffers from the larger CPU time in finite element analyses [9]. Besides the Hill's family, there were also different yield functions proposed in the literature. Gotoh developed the first polynomial-based yield function, which overcomes the anomalous issues [10], but this criterion could not provide the convexity conditions for several aluminum alloys [11]. Barlat and Lian proposed a non-quadratic yield function considering the planar anisotropy (Barlat-89) [12]. This linear transformation-based yield function is quite practical for aluminum alloys without high anisotropic behavior, but it cannot be used for three-dimensional stress state. For the three-dimensional stress state, Barlat et al. proposed another yield criterion based on linear transformation [13]. However, this criterion only predicts the directionality of the yield stress ratios. Then Barlat et al. developed Yld91 criterion and proposed Yld96 criterion, which predicts both angular variations of the r values and yield stress ratios [14]. Later, Barlat et al. proposed a sophisticated yield criterion named Yld2000-2d based on two linear transformations for plane stress state. This criterion predicts both the angular variations of r values and yield stress ratios simultaneously. In addition, this criterion considers the biaxial yield stress and r-value [15]. There were also different non-quadratic yield criteria in the literature [16–18]. Most of the yield functions mentioned hitherto are embedded into the finite element (FE) codes, or their implementation procedures into FE software are not difficult. Correspondingly, applicability of different yield criteria on different steel grades and aluminum alloys was evaluated. Toros et al. [19] investigated the performance of Hill48, Yld89, and Yld2000-2d on the spring-back behavior of TRIP800 steel. Xu et al. [20] carried out hole expansion tests of a TWIP steel sheet and numerical simulations of these tests using the Yld2000-2d yield criterion. For both studies, Yld2000-2d provided accurate results. Kuwabara et al. [21] conducted a similar work and used Hill48 and Yld2000-2d as yield criteria for AA6016-O and AA6016-T4 aluminum alloys. They reported that the numerical results obtained from Yld2000-2d were in accordance with the experimental results.

With the development of computer science, mechanical tests can be simulated using the FE method with minimum cost. However, anisotropy parameters based on the r value and the yield stress ratio directionalities are directly obtained from analytical methods and yield criteria related to the computed anisotropy parameters were implemented into the FE software.

When yield criteria are implemented into the finite element software, it is uncertain that the FE software could reflect the anisotropic behavior of the material and capture the analytical input values completely. It should be also investigated that the FE model could capture the anisotropic behavior of the material and assess the analytical model accurately.

From this perspective, in the present study, the differences between the analytical and numerical predictions of the r value and the yield stress ratios directionalities were evaluated. To this end, a single finite element was modeled to perform the simulations. Two materials widely used in the automotive industry, namely DP600 and AA2090-T3 aluminum alloy were investigated. Uniaxial tensile test conditions were applied on the single finite element. Lankford parameters and the yield stress ratios were determined for different material orientations using simulations. Numerical and analytical predictions are validated with experimental results.

2 Materials and method

Dual-phase (DP) steels are widely used steels among the AHSS and show not only adequate strength but also high ductility. These steels contain martensite grains surrounded by a ferrite matrix [22–24]. Ferrite matrix ensures ductility, whereas martensite islands ensure sufficient strength [22]. On the other hand, aluminum alloys show low ductility, and they

are inclined to fracture during the deformation processes [21]. Moreover, several aluminum alloys demonstrate significant anisotropy [25, 26].

In this study, dual-phase DP600 steel and 2090-T3 aluminum alloy were used to present plasticity model capabilities for predictive modeling based on directionalities of both yield stress ratios and anisotropy coefficients. Hill-48, Barlat-89, and Yld2000-2d yield criteria were performed to exhibit the predictive modeling capability of commonly used plasticity models.

3 Plasticity models

3.1 Hill-48 criterion

Hill (1948) yield function is given in following equation [2].

$$2f = F\left(\sigma_{yy}-\sigma_{zz}\right)^2 + G\left(\sigma_{zz}-\sigma_{xx}\right)^2 + H\left(\sigma_{xx}-\sigma_{yy}\right)^2 + 2L\tau_{yz}^2 + 2M\tau_{zx}^2 + 2N\tau_{xy}^2 = 1 \tag{1}$$

Here, F, G, H, L, M, and N are the anisotropy parameters to be calibrated. These parameters were calculated through Lankford parameters as in the following equations.

$$\mathrm{F} = \frac{r_0}{r_{90}\left(1+r_0\right)} \tag{2}$$

$$\mathrm{G} = \frac{1}{1+\mathrm{r}_0} \tag{3}$$

$$\mathrm{H} = \frac{r_0}{\left(1+r_0\right)} \tag{4}$$

$$\mathrm{N} = \frac{\left(r_0+r_{90}\right)\left(1+2r_{45}\right)}{2r_{90}\left(1+r_0\right)} \tag{5}$$

3.2 Barlat-89 criterion

Barlat (1989) yield criterion Φ for plane stress is defined as [12]:

$$\Phi = a\left|K_1+K_2\right|^m + a\left|K_1-K_2\right|^m + c\left|2K_2\right|^m = 2\sigma_Y^m \tag{6}$$

where σ_Y is the yield stress and $K_{i=1,2}$ are given by:

$$K_1 = \frac{\sigma_x + h\sigma_y}{2} \tag{7}$$

$$K_2 = \sqrt{\left(\frac{\sigma_x - h\sigma_y}{2}\right)^2 + p^2\tau_{xy}^2} \tag{8}$$

The anisotropic material constants a, c, h, and p are obtained through R_{00}, R_{45}, and R_{90}:

$$a = 2 - 2\sqrt{\left(\frac{R_{00}}{1+R_{00}}\right)\left(\frac{R_{90}}{1+R_{90}}\right)} \tag{9}$$

$$c = 2 - a \tag{10}$$

$$h = \sqrt{\left(\frac{R_{00}}{1+R_{00}}\right)\left(\frac{1+R_{90}}{R_{90}}\right)} \tag{11}$$

3.3 Yld2000-2d criterion

The yield condition for Yld2000-2d criterion can be written [15]

$$f\left(\sigma,\alpha,\varepsilon_p\right) = \sigma_{eff}\left(\sigma_{xx}-2\alpha_{xx}-\alpha_{yy},\sigma_{yy}-2\alpha_{yy}-\alpha_{xx},\sigma_{xy}-\alpha_{xy}\right) - \sigma_Y^t\left(\varepsilon_p,\dot{\varepsilon}_p,\beta\right) \le 0 \tag{12}$$

where

$$\sigma_{eff}\left(S_{xx},S_{yy},S_{xy}\right) = \left[\frac{1}{2}\left(\varphi'+\varphi''\right)\right]^{1/a} \tag{13}$$

$$\varphi' = \left|X_1'-X_2'\right|^a \tag{14}$$

$$\varphi'' = \left|2X_1''+X_2''\right|^a + \left|X_1''+2X_2''\right|^a \tag{15}$$

The X_i' and X_i'' are eigenvalues of X_{ij}' and X_{ij}'' and are given by

$$X_1' = \frac{1}{2}\left(X_{11}'+X_{22}'+\sqrt{\left(X_{11}'-X_{22}'\right)^2+4X_{12}'^2}\right) \tag{16}$$

$$X_2' = \frac{1}{2}\left(X_{11}'+X_{22}'-\sqrt{\left(X_{11}'-X_{22}'\right)^2+4X_{12}'^2}\right) \tag{17}$$

and

$$X_1'' = \frac{1}{2}\left(X_{11}''+X_{22}''+\sqrt{\left(X_{11}''-X_{22}''\right)^2+4X_{12}''^2}\right) \tag{18}$$

$$X_2'' = \frac{1}{2}\left(X_{11}''+X_{22}''-\sqrt{\left(X_{11}''-X_{22}''\right)^2+4X_{12}''^2}\right) \tag{19}$$

respectively. The X_{ij}' and X_{ij}'' are given by

$$\begin{pmatrix} X_{11}' \\ X_{22}' \\ X_{12}' \end{pmatrix} = \begin{pmatrix} L_{11}' & L_{12}' & 0 \\ L_{21}' & L_{22}' & 0 \\ 0 & 0 & L_{33}' \end{pmatrix} \begin{pmatrix} S_{xx} \\ S_{yy} \\ S_{xy} \end{pmatrix} \tag{20}$$

$$\begin{pmatrix} X''_{11} \\ X''_{22} \\ X''_{12} \end{pmatrix} = \begin{pmatrix} L''_{11} & L''_{12} & 0 \\ L''_{21} & L''_{22} & 0 \\ 0 & 0 & L''_{33} \end{pmatrix} \begin{pmatrix} S_{xx} \\ S_{yy} \\ S_{xy} \end{pmatrix} \tag{21}$$

where,

$$\begin{pmatrix} L'_{11} \\ L'_{12} \\ L'_{21} \\ L'_{22} \\ L'_{33} \end{pmatrix} = \frac{1}{3} \begin{pmatrix} 2 & 0 & 0 \\ -1 & 0 & 0 \\ 0 & -1 & 0 \\ 0 & 2 & 0 \\ 0 & 0 & 3 \end{pmatrix} \begin{pmatrix} \alpha_1 \\ \alpha_2 \\ \alpha_7 \end{pmatrix} \tag{22}$$

$$\begin{pmatrix} L''_{11} \\ L''_{12} \\ L''_{21} \\ L''_{22} \\ L''_{33} \end{pmatrix} = \frac{1}{9} \begin{pmatrix} -2 & 2 & 8 & -2 & 0 \\ 1 & -4 & -4 & 4 & 0 \\ 4 & -4 & -4 & 1 & 0 \\ -2 & 8 & 2 & -2 & 0 \\ 0 & 0 & 0 & 0 & 9 \end{pmatrix} \begin{pmatrix} \alpha_3 \\ \alpha_4 \\ \alpha_5 \\ \alpha_6 \\ \alpha_8 \end{pmatrix} \tag{23}$$

The parameters α_1 to α_8 are the parameters that determine the shape of the yield surface.

4 Application study

In this study, directionalities of both yield stress ratios and anisotropy coefficients (r) were predicted analytically and numerically using Hill-48, Barlat-89, and Yld2000-2d criteria. In the first stage of the study plasticity model parameters of DP600 and AA 2090-T3 materials were identified using the uniaxial tensile test results for 7 directions varying from rolling direction (0°) to transverse direction (90°) at 15° degree intervals in Refs. [27] and [28]. Uniaxial tensile tests were conducted based on ASTM-E8 standard [29] with 1 mm and 1.6 mm gauge thickness for DP600 and AA2090-T3, respectively (Fig. 1).

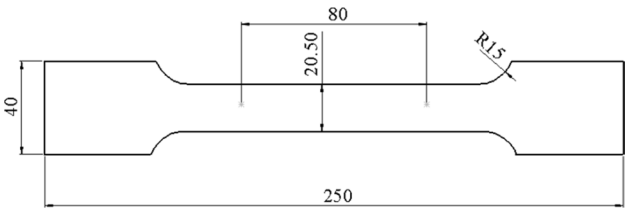

Fig. 1 ASTM-E8 uniaxial tensile test sample dimensions

Plasticity model parameters of these materials are summarized in Table 1. Using these parameters analytical predictive modeling is performed for all plasticity models to obtain angular variations of yield stress ratios and anisotropy coefficients. In the analytical modeling stage, plasticity model equations were implemented into a Matlab code and yield stress ratio and anisotropy coefficient predictions were performed by using plasticity model material inputs, and angular variations were observed for all materials.

In the numerical modeling stage of the study, finite single element test was used to identify the prediction capacity of the plasticity models. For this purpose, a single shell element is generated by using Belystchko-Tsay [30] element formulation with 7 integration points through the thickness. Ls-Dyna commercial software was used in the finite element analyses. Boundary conditions were applied as summarized in Fig. 2. Tensile tests in 7 directions until 0.2 strain values in 1 s were performed to obtain the yield stress ratios and r values.

5 Results & discussion

In this section comparison results of analytical and numerical predictions of the plasticity models with experimental validation were presented. Firstly, stress–strain curves of the single finite element tests are obtained, and these curves can be seen in Fig. 3 and Fig. 4, for DP600 and 2090-T3 aluminum alloy materials, respectively. In all figures, 0° represents the rolling direction, while 90° represents transverse direction. It can be seen that the effect of the anisotropy was captured by all plasticity models for both materials.

It was observed from Fig. 5 and Fig. 6 that analytical and numerical yield stress ratio predictions in the same material orientations were in accordance with each other for all criteria and materials. Nevertheless, several deviations in the predictions of r value directionalities were observed in certain angular intervals for both materials. Finally, comparisons

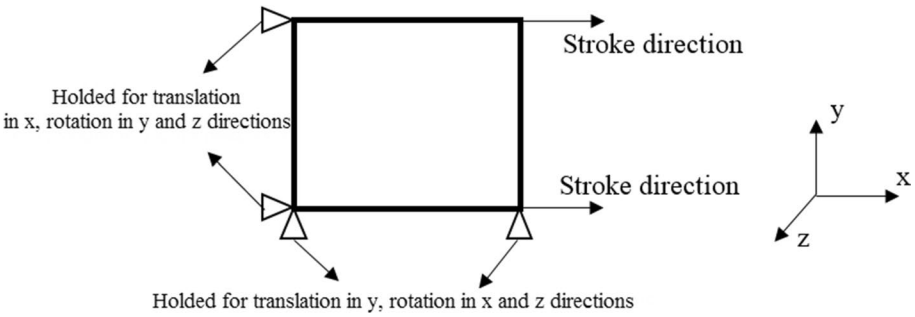

Fig. 2 Boundary conditions of the single finite element test

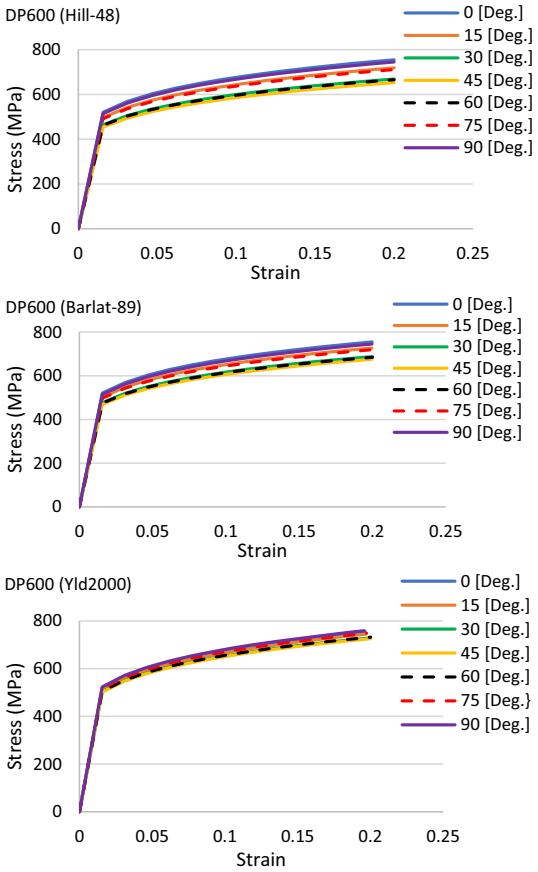

Fig. 3 Stress–strain curves obtained by single finite element test for DP600

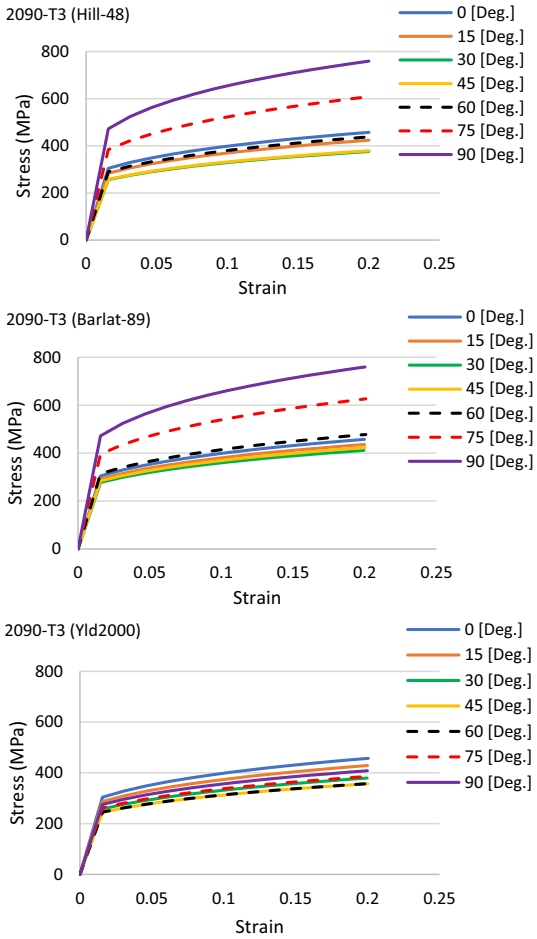

Fig. 4 Stress–strain curves obtained by single finite element test for 2090-T3 In the next stage, angular variations of yield stress ratios and anisotropy coefficients (r) were compared using analytical and numerical approaches. Comparison results can be seen in Fig. 5 and Fig. 6.

between analytical and numerical results were presented to identify the difference between the approaches more clear. These results can be seen in Fig. 7 and Fig. 8.

Numerical predictions of the yield stress ratio and r value directionalities of the Hill-48 yield function were compatible with the analytical predictions for both materials. Solely, numerical predictions overestimated the r values in comparison to the analytical results between 45° and 90° for 2090-T3 aluminum alloy. On the other hand, Barlat-89 and Yld2000-2d criteria exhibited similar behaviors for DP600 steel and numerical results obtained from these criteria underestimated the r values compared to the analytical results. Regarding the 2090-T3 aluminum alloy, numerical predictions obtained from Yld2000-2d criterion were in good agreement with the analytical results. Barlat-89 showed similar behaviors with Hill-48 criterion, and it was seen that the numerical results of Barlat-89 predicted higher r values between 45° and 90° when compared to the analytical results. For Barlat-89 and Yld2000-2d criteria, numerical predictions of yield stress ratios were consistent with the analytical results similar to the Hill-48 criterion for both materials. Moreover, it was observed for 2090-T3 that the differences between the numerical and analytical results were lower than DP600 steel.

6 Conclusions

In this study, it is aimed to present the differences between the analytical and numerical predictions of the yield stress ratios and Lankford parameters directionalities for anisotropic materials to clarify the implementation accuracy of commonly used plasticity models. For this purpose, three different plasticity models were used as Hill-48, Barlat-89, and Yld2000-2d. Two materials widely used in the automotive industry, namely DP600 and AA2090-T3 were studied. Uniaxial tensile tests by 7 directions for these materials with single finite element tests were performed for numerical predictions. Ls-Dyna commercial finite element software

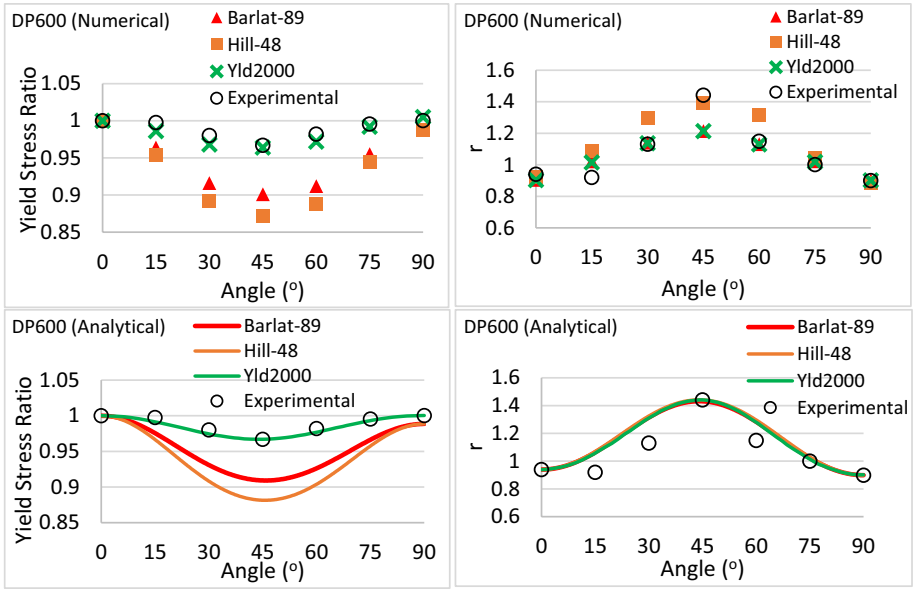

Fig. 5 Angular variations of yield stress ratios and anisotropy coefficients (r) obtained by analytical and numerical approaches for DP600

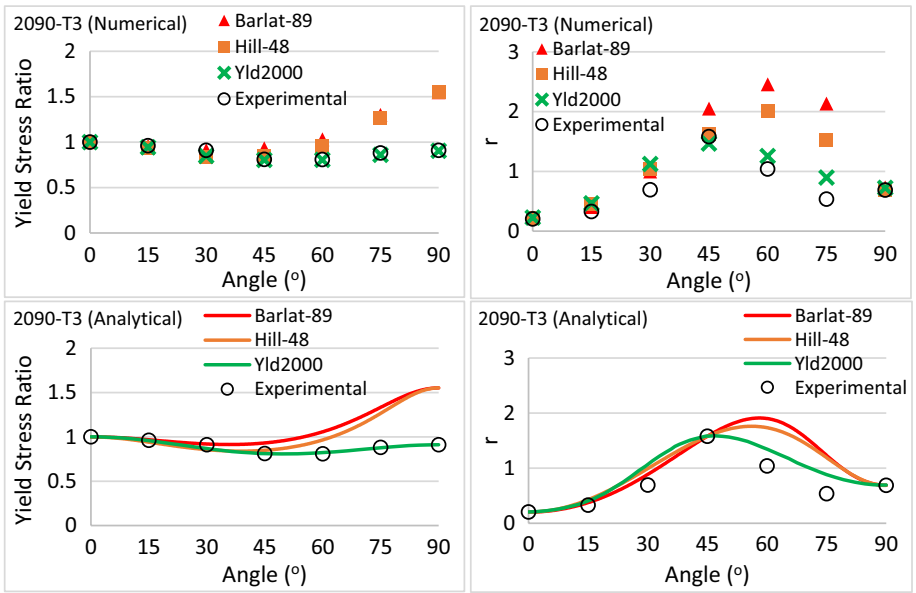

Fig. 6 Angular variations of yield stress ratios and anisotropy coefficients (r) obtained by analytical and numerical approaches for 2090-T3

was used in finite element analyses. Plasticity models were implemented into Matlab codes for analytical predictions.

Numerical stress–strain curves of the materials were determined and compared based on angular variations. It is seen that all plasticity models were captured the anisotropy effect. Then, the yield stress ratios and Lankford parameters were obtained for different material orientations using finite element predictions and compared with the analytical results. It is observed that analytical and numerical yield stress ratio predictions in the same material orientations have an agreement with each other for all plasticity models and materials. Nevertheless, several deviations in the predictions of r value directionalities were observed in certain angular intervals for both materials. Numerical predictions of the yield stress ratio and r value directionalities of the Hill-48 yield function were compatible with the analytical predictions for both materials. On the other hand, Barlat-89 and Yld2000-2d criteria exhibited similar behaviors for DP600 steel and numerical results obtained from these criteria underestimated the r values compared to the analytical results. Regarding the 2090-T3 aluminum alloy, numerical predictions obtained from Yld2000-2d criterion were in good agreement with the analytical results while Barlat-89 showed similar behaviors with Hill-48 criterion, and it was seen that the numerical results of Barlat-89 predicted higher r values between 45° and 90° when compared to the

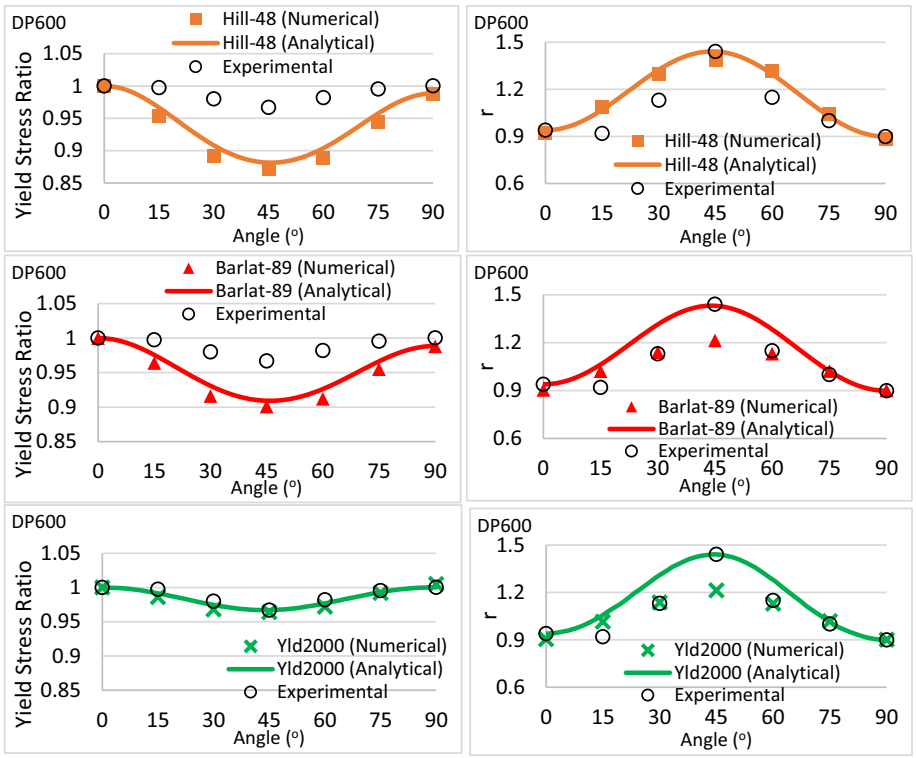

Fig. 7 Comparison of analytical and numerical approaches prediction results for DP600

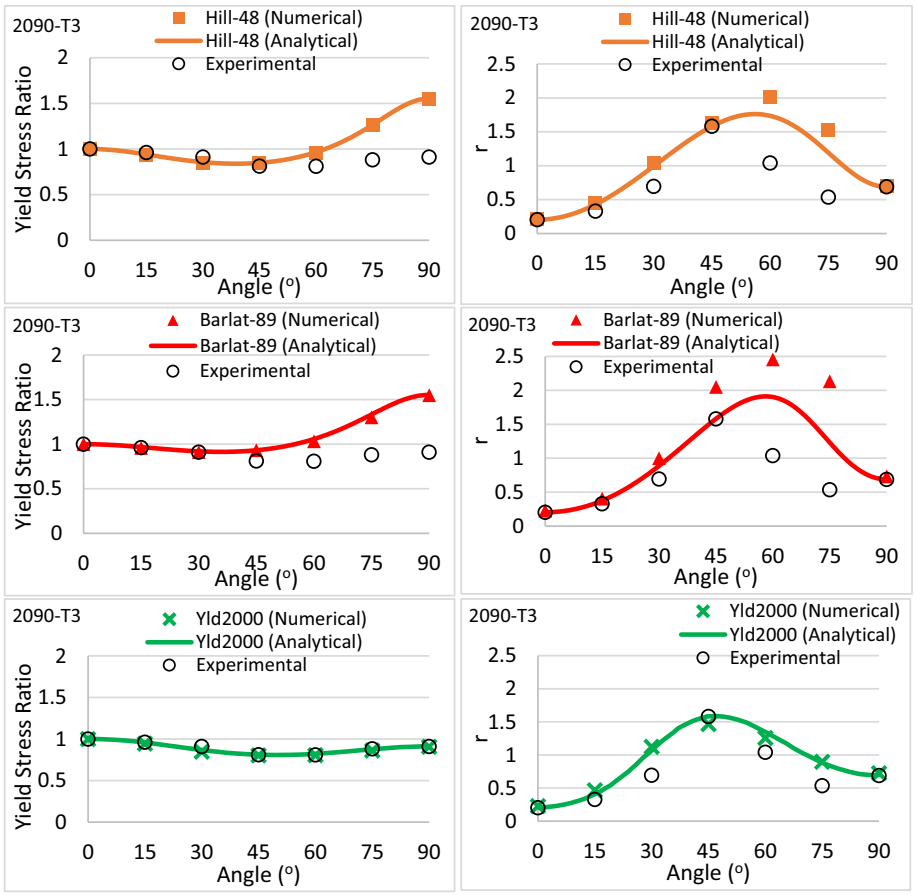

Fig. 8 Comparison of analytical and numerical approaches prediction results for 2090-T3

Table 1 Plasticity model parameters of the materials used in this study

Hill-48 Criterion									
	F		G		H		N		
DP600	0.539		0.516		0.484		2.047		
2090-T3	0.246		0.831		0.169		2.239		
Barlat-89 Criterion									
	a		c		h		p		m
DP600	1.042		0.958		1.012		1.130		6
2090-T3	1.475		0.525		0.644		1.170		8
Yld2000-2d Criterion									
	α_1	α_2	α_3	α_4	α_5	α_6	α_7	α_8	a
DP600	1.055	0.940	0.990	1.006	1.033	1.184	1.070	0.943	6
2090-T3	0.488	1.377	0.754	1.025	1.036	0.904	1.231	1.485	8

analytical results. For Barlat-89 and Yld2000-2d criteria, numerical predictions of yield stress ratios were consistent with the analytical results similar to the Hill-48 criterion for both materials. Moreover, it was observed for 2090-T3 alloy that the differences between the numerical and analytical results were lower than DP600 steel.

It is concluded that the implementation of the Hill-48 criterion is quite successful. However, Barlat yield functions family has significant strength and deformation differences between analytical and numerical results, especially for steel sheets.

Funding Not applicable

Declarations

Conflicts of interest The author's declared that they have no conflict of interest.

References

1. Firat M (2008) A numerical analysis of sheet metal formability for automotive stamping applications. Comput Mater Sci. https://doi.org/10.1016/j.commatsci.2008.01.068
2. Hill R (1948) A theory of the yielding and plastic flow of anisotropic metals. Proc R Soc London Ser A. https://doi.org/10.1098/rspa.1948.0045
3. Chung K, Ma N, Park T, Kim D, Yoo D, Kim C (2011) A modified damage model for advanced high strength steel sheets. Int J Plast. https://doi.org/10.1016/j.ijplas.2011.01.007
4. Woodthrope J, Pearce R (1970) The anomalous behavior of aluminum sheet under balanced biaxial tension. Int J Mech Sci. https://doi.org/10.1016/0020-7403(70)90087-1
5. Banabic D, Müller W, Pöhlandt K (1998) Determination of yield loci from cross tensile tests assuming various kinds of yield criteria. Sheet Metal Forming Beyond 2000, Brussels, Belgium
6. Hill R (1979) Theoretical plasticity of textured aggregates. Math Proc Cambridge Philos Soc. https://doi.org/10.1017/S0305004100055596
7. Hill R (1990) Constitutive modelling of orthotropic plasticity in sheet metals. J Mech Phys Solids. https://doi.org/10.1016/0022-5096(90)90006-P
8. Hill R (1993) A user-friendly theory of orthotropic plasticity in sheet metals. Int J Mech Sci. https://doi.org/10.1016/0020-7403(93)90061-X
9. Banabic D (2010) Sheet metal forming processes constitutive modelling and numerical simulation, Cluj–Napoca, Romania
10. Gotoh M (1977) A theory of plastic anisotropy based on a yield function of fourth order (plane stress state). Int J Mech Sci. https://doi.org/10.1016/0020-7403(77)90043-1
11. Soare SC (2007) On the use of homogeneous polynomials to develop anisotropic yield functions with applications to sheet forming. Dissertation, University of Florida
12. Barlat F, Lian J (1989) Plastic behavior and stretchability of sheet metals part 1 a yield function for orthotropic sheets under plane stress conditions. Int J Plast. https://doi.org/10.1016/0749-6419(89)90019-3
13. Barlat F, Lege DJ, Brem JC (1991) A six component yield function for anisotropic materials. Int J Plast. https://doi.org/10.1016/0749-6419(91)90052-Z
14. Yoon JW, Barlat F, Chung K, Pourboghrat F, Yang DY (2000) Earing predictions based on asymmetric nonquadratic yield function. Int J Plast. https://doi.org/10.1016/S0749-6419(99)00086-8
15. Barlat F, Brem JC, Yoon JW, Chung K, Dick RE, Lege DJ, Pourboghrat F, Choi SH, Chu E (2003) Plane stress yield function for aluminum alloy sheets—part 1: theory. Int J Plast. https://doi.org/10.1016/S0749-6419(02)00019-0
16. Hershey AV (1954) The plasticity of an isotropic aggregate of anisotropic face centered cubic cyristal. J Appl Mech ASME 21:241–249
17. Hosford WF (1979) On yield loci of anisotropic cubic metals. In: Proceedings of the 7th North American Metalworking Conference (NMRC) Dearborn, 191–197
18. Bassani JL (1977) Yield characterization of metals with transversaly isotropic plastic properties. Int J Mech Sci. https://doi.org/10.1016/0020-7403(77)90070-4
19. Toros S, Polat A, Oztırk F (2012) Study on the definition of equivalent plastic strain under non-associated flow rule for finite

element formulation. Mater Des. https://doi.org/10.1016/j.matdes.2012.05.006
20. Xu L, Barlat F, Lee MG (2012) Hole expansion of twinning-induced plasticity steel. Scripta Materilia. https://doi.org/10.1016/j.scriptamat.2012.01.062
21. Kuwabara T, Mori T, Asano M, Hakoyama T, Barlat F (2017) Material modeling of 6016-O and 6016–T4 aluminum alloy sheets and application to hole expansion forming simulation. Int J Plast. https://doi.org/10.1016/j.ijplas.2016.10.002
22. Alaie A, Kadkhodapour J, Rad SZ, Asadabad MA, Schmauder S (2015) Formation and coalescence of strain localized regions in ferrite phase of DP600 steels under uniaxial tensile deformation. Mater Sci & Eng A. https://doi.org/10.1016/j.msea.2014.11.042
23. Aşık EE, Perdahçıoğlu PS, van den Boogard AH (2019) Microscopic investigation of damage mechanisms and anisotropic evolution of damage in DP600. Mater Sci & Eng A. https://doi.org/10.1016/j.msea.2018.10.018
24. Darabi AC, Guski V, Butz A, Kadkhodapour J, Schmauder SA (2020) Comparative study on mechanical behavior and damage scenario of DP600 and DP980 steels. Mech of Mater. https://doi.org/10.1016/j.mechmat.2020.103339
25. Hu Q, Li X, Han X, Li H, Chen J (2017) A normalized stress invariant-based yield criterion: Modeling and validation. Int J Plast. https://doi.org/10.1016/j.ijplas.2017.09.010
26. Hu Q, Li X, Chen J (2017) On the calculation of plastic strain by simple method under nonassociated flow rule. Europ J Mech A/Solids. https://doi.org/10.1016/j.euromechsol.2017.08.017
27. Pham QT, Lee MG, Kim YS (2021) New procedure for determining the strain hardening behavior of sheet metals at large strains using the curve fitting method. Mech of Mater. https://doi.org/10.1016/j.mechmat.2020.103729
28. Safaei M, Yoon JW, De Waele W (2014) Study on the definition of equivalent plastic strain under non-associated flow rule for finite element formulation. Int J Plast. https://doi.org/10.1016/j.ijplas.2013.09.010
29. Standard ASTM (2011) E8/E8M. Stand. test meth. Tens. Test. Metal. Mater. 3:66
30. Belytschko T, Lin JI, Chen-Shyh T (1984) Explicit algorithms for the nonlinear dynamics of shells. Comp Met App Mech Eng. https://doi.org/10.1016/0045-7825(84)90026-4